Evaluating and Extending the Arctic Monitoring and Assessment Programme (AMAP) Climate Emulator

Supervisors: Paul Kushner and Knut von Salzen

Student: Victoria Spada

Student Number: 1005254868

January 30, 2023

Contents

List of Figures

List of Tables

1 Introduction

Computational Earth System Models (ESMs) are used to simulate projected warming, climate change, and air quality scenarios. However, they are computationally expensive, which may not be suitable for climate and air quality assessments in which the effects of multiple pollutants are considered. Climate emulators and air quality source-receptor models employ analytic relationships between emissions, concentrations, and radiative forcing, using inexpensive models that highly approximate, parametrize, and even linearize, the impacts of Earth's complex physical and chemical processes [1], [2]. Short-lived climate forcers (SLCFs) are a group of greenhouse gases (GHGs) and other pollutants that have relatively short atmospheric lifetimes (compared to carbon dioxide (CO_2) and can greatly impact climate change and air quality [3]. Due to their short lifetimes and trace amounts, which result in high uncertainties even in ESMs, emulators are a computationally inexpensive and effective tool for SLCF science in support of climate and air quality policy development [1], [3], [4].

The Arctic Monitoring and Assessment Programme (AMAP) Air Quality and Climate Emulator (hereafter referred to as the AMAP emulator) uses a greatly simplified ESM to predict changes in air quality and climate in five regions based on regional anthropogenic emissions of air pollutants and GHGs, including SLCFs. The tool is new and has the potential for tuning, extension, and numerous applications in climate science and policy. However, the emulator has limitations [1].

One important limitation of the AMAP emulator relates to Arctic amplification, which refers to the enhancement of changes in surface air temperature over the Arctic relative to lower latitudes [5]. The emulator has been found to underestimate Arctic amplification when compared to Coupled Model Intercomparison Project Phase 6 (CMIP6) ESMs [1], [6].

Additionally, methane (CH_4) is treated as a well-mixed GHG without spatial structure in radiative forcings or dependence on regional emission sources. Uncertainties in Arctic temperature projections resulting from uncertainties in natural CH_4 emissions are high because the emulator lacks an estimate of future natural emissions [1].

The purpose of this study is to better characterize and address the limitations of the AMAP emulator. First, the emulator's output is reviewed and evaluated, with a focus on

analyzing and tuning the climate output of the emulator in the Arctic for different emissions scenarios [7], [8].

CH_4 is modelled in the emulator as a well-mixed forcer, so to address this limitation, its atmospheric lifetime will be tweaked. Natural emissions of CH_4 will also be incorporated into the emulator as a linear feedback from temperature to account for the potential increase in anaerobic respiration as a natural methane source [9] [10]. The emulator will be run with different CH_4 emissions to observe how different scenarios affect regional and global temperatures. Finally, the AMAP emulator will be used to quantify the effects of black carbon (BC) as an SLCF on Arctic climatology [11].

2 Literature Review

This literature review begins with a more in-depth introduction to SLCFs and their impacts on global climate change and health, and how they motivate climate emulation. Then, recent intercomparison studies of ESMs and RCMs are explored, and some state-of-the-art climate emulators are reviewed. The AMAP emulator is outlined in detail. Finally, results of studies involving the AMAP emulator that motivate the goals of the study are discussed.

2.1 Climate Change and Short-lived Climate Forcers

SLCFs can greatly contribute to global warming and impact air quality. Some of the key SLCFs are BC, CH_4, organic carbon (OC), tropospheric ozone (O_3), and hydrofluorocarbons (HFCs). They are emitted by a variety of sources and have a wide range of climate impacts [3], [4], [12].

CH_4 is a GHG with a high radiative efficiency. Since it has an atmospheric lifetime of about 12 years, which is relatively high compared to other SLCFs, it is sometimes considered a well-mixed GHG as opposed to a SLCF. It affects air quality as a precursor to tropospheric O_3, and also acts a precursor to stratospheric water vapour, another GHG [4], [9], [12], [13].

O_3 is an air pollutant and GHG that forms in the stratosphere when sunlight interacts with its precursor gases, such as CH_4, CO, non-CH_4 volatile organic compounds (NMVOCs) and nitrogen oxides (NO_x) [4], [12]. Its atmospheric lifetime ranges from hours in urban

areas to up to weeks or months in the upper troposphere [13].

Sulfate aerosols form from sulfur compound emissions and account for a lot of PM2.5 (fine particles in the atmosphere with a diameter ≤ 2.5 μm). They efficiently scatter sunlight and increase the albedo of clouds, causing less solar radiation to reach Earth's surface. This results in cooling that counteracts the warming effects of other SLCFs and GHGs [4], [12]. The impacts clouds are an important source of uncertainty in climate modelling [14]. With globally declining levels of sulfate aerosols in the past three decades, the masking effect of these aerosols on global warming is diminishing, which enhances warming in the Arctic and globally [3], [4], [15].

BC and OC are also SLCFs that contribute to global warming and can degrade air quality. BC decreases the albedo of snow when deposited over top it, and it is thus an important SLCF in Arctic climatology [3], [11], [16].

In addition to combating global warming, reducing emissions of SLCFs can improve human health globally. Atmospheric O_3 and particulate matter have been linked with an increased risk for respiratory disease, premature death, and other adverse health outcomes [4], [17], [18], [19]. SLCFs can degrade air quality and contribute to climate change, and though these topics are often considered separately, there are strong links between them, as evidenced by recent studies [20] [21], [22].

2.2 Evaluating ESMs and Climate Emulators

In 2020, the Reduced Complexity Model Intercomparison Project (RCMIP) was launched to mirror CMIP (Coupled Model Intercomparison Project), a global project which examines numerous cutting-edge comprehensive ESMs and Atmosphere-Ocean General Circulation Model (AOGCMs) [2]. RCMIP uses scenario-based and idealized scenarios to study simulated global-mean temperature responses from various climate emulators, or RCMs.

CMIP is an major project in the realm of climate modelling and climate change, as by evaluating and comparing the output for plausible emissions scenarios with cutting-edge ESMs, a better understanding of climate change can be attained. The current generation of CMIP6 ESMs was found to produce the greatest range of equilibrium climate sensitivity (ECS) values of any phase to date, ranging from 1.8 to 5.6°C, a range derived from 37

models. The ECS is a commonly used parameter in Earth system modelling that quantifies the global surface temperature response associated with doubling Earth's atmospheric CO_2 concentration [14]. This is the largest range of ECS values estimated for any generation of ESMs [14], [23].

RCMs are highly valuable for their low computational costs, high speed, and good estimation abilities, so the establishment of an ongoing comprehensive evaluation and assessment of RCMs is of interest. As of January 2023, two phases of RCMIP have been conducted, with a third phase currently in progress [2], [24].

Phase 1 of RCMIP defined its experiments with species concentrations to facilitate a direct comparison with CMIP experiments, which use Shared Socioeconomic Pathways (SSPs). SSPs are plausible scenarios of global anthropogenic development that would results in different challenges in mitigating climate change [25]. Specifically, there are five umbrella narratives for socio-economic development: sustainable development (SSP1), middle-of-the-road development (SSP2), regional rivalry (SSP3), inequality (SSP4), and fossil-fueled development (SSP5).

The primary difference between the RCMIP and CMIP experiments is that RCMs often incorporate more antropogenic driver species, such as all of the hydrofluorocarbon (HFC), fluorocarbon (PFC), and hydrochlorofluorocarbon (HCFC) species, and aerosols precursors [2].

In addition to valuable intercomparison, RCMIP enables comparisons with complex models by using similar, and some identical scenarios used in CMIP. Quantifying how much the simplifications in RCMs reduces their competence to replicate forcing and temperature responses from complex models ists crucial to evaluating their utility. Phase 1 of RCMIP showed that RCMs were able to capture the temperature responses of CMIP5 and CMIP6 models within a root mean-square error of 0.2 $\circ$C [2].

2.3 A Survey of Climate Emulators

While climate emulators are much simpler than comprehensive ESMs, they have been able to reproduce forced temperature trends simulated by ESMs within the uncertainty of the ESM simulations for many scenarios [1], [26], [27], [28], [29], [30] , [31]. Additionally, source-

receptor models have been used to simulate the effects of numerous emissions scenarios on global air quality 1], [32], [33], [34], [35], [36].

The following is a survey of some recent climate emulators that were included in RCMIP Phase 1. Some key similarities and differences between these emulators, as well as the AMAP emulator, are shown in Table 1.

The OSCAR v2.2 emulator [31] is a climate emulator that models emissions with an impulse response, which is commonly used in climate emulators [2], [24], [30],[31], [37]. The climate model includes the oceanic and terrestrial carbon cycles to simulate atmospheric CO_2, tropospheric chemistry and natural wetlands to simulate atmospheric CH_4 and O_3, stratospheric chemistry to simulate NO and O_3, 37 halogenated compounds, dynamic surface albedo due to BC deposited on snow and land cover changes, and the resulting effects on aerosols. The forcing due to anthropogenic emissions incorporates CO_2 from burning fossil fuels and cement production, CH_4, NO, halogenated compounds, CO, NMVCs, SO2, NH_4, BC, and OC [31].

The FaIR v1.1 emulator an emmissions-based climate emulator that also models emissions as an impulse response [30]. It has a global resolution and computes atmospheric concentrations of GHGs, outputting the resulting concentrations and effective radiative forcings (ERF) of these greenhouse gases, as well as aerosols, O_3 precursors and other agents. It includes a total of 13 forcing agents: CO_2, CH_4, N_2O, other GHGs, tropospheric O_3, stratospheric O_3, stratospheric water vapour, contrails, aerosols, BC on snow, land use change, and volcanic and solar activity.

The ERFs are used to calculate the global mean surface temperature change. The calculated change in temperature is then incorporated into a carbon cycle feedback, impacting the atmospheric lifetime of carbon dioxide [30].

The MAGICC emulator is an AOGCM consisting of a hemispherically averaged upwelling diffusion ocean coupled with a globally averaged carbon cycle model and an atmosphere layer [26]. It includes radiative forcings due to CO_2, CH_4, NO, tropospheric aerosols, tropospheric and stratospheric O_3, and various halogenated gases. This emulator, along with the others in this review, has a temporal resolution of 1 year. As with many other climate emulators, the equilibrium climate sensitivity is a primary model parameter [26], [2].

Table 1: Survey of recent climate emulators.

Model	Spatial Resolution	Forcing Agents	Climate Response to Radiative Forcing
AMAP	4 latitude bands (60°N-90°N, 28°N-60°N, 28°S-28°S, and 90°S-28°S)	CH_4, OC, BC, sulfate, O_3, CO_2	Modified impulse response
FaIR v1.1	Global	CO_2, CH_4, N_2O, other GHGs, stratospheric and tropospheric O_3, stratospheric water vapour, contrails, aerosols, BC, land use change, and volcanic and solar activity	Modified impulse response
MAGICC	Hemispheric land/ocean	CO_2 (including terrestrial and ocean carbon cycles and athropogenic emissions), CH_4, NO, tropospheric aerosols, tropospheric and stratospheric O_3, and various halogenated gases	Atmospheric energy balance model with 50-layer upwelling diffusion- entrainment ocean
OSCAR v2.2	Global with regionalised carbon cycle	oceanic and terrestrial carbon cycles (CO_2), tropospheric chemistry and natural wetlands to simulate atmospheric (CH_4, O_3), stratospheric chemistry NO and O_3, 37 halogenated compounds, dynamic surface albedo due to BC deposited on snow and changes in land cover, and aerosols. Anthropogenic emissions incorporate CO_2 from burning fossil fuels and cement production, CH_4, NO, halogenated compounds, CO, NMVCs, SO_2, NH_4, BC, and OC	Impulse Response

The time-varying ECS is defined using the transient energy balance equation defined for a perturbed climate system. The MAGICC carbon cycle can emulate temperature-feedback effects on the heterotrophic respiration carbon fluxes.

2.4 The AMAP Air Quality and Climate Emulator

AMAP is an Arctic Council Working Group that studies and reports on the status of and threats to the Arctic environment. AMAP provides advice on political actions that would assist Arctic governments in the remediation and prevention of climate change [38].

The AMAP emulator is a climate and air quality emulator that simulates relationships between Earth's air quality, emissions. and climate. The emulator focuses on SLCFs because of their significant impact on Arctic climate and air quality [3], [4], [9], [11]. It includes emissions of CO_2, CH_4, CO, NO_x, volatile organic compounds (VOCs), S, BC, and OC. Since no other climate forcers are considered, warming simulations are probably underestimated by the AMAP emulator [1].

The emulator runs over 4 latitude bands: 60°N to 90°N (Arctic), 28°N to 60°N (Northern Hemispheric mid-latitudes), 28°S to 28°S (tropics), and 90°S to 28°S (Southern Hemisphere mid-latitudes and Antarctica). The main climate outputs of the emulator are the regional and global temperature perturbation responses [1].

The climate response to pulse emissions of various species is simulated using a highly approximated, linearized mass and energy balance system for Earth. The emulator simulates Earth's average surface air temperature response when forced by a series of instantaneous pulse emissions of different species, which affect the energy balance of the climate system by changing radiative forcings of greenhouse gases and SLCFs. The AMAP emulator simulates the temporal evolution of the 4 outputted regional mean temperatures using a specified climate sensitivity, time scales of heat dissipation, and Regional Temperature-Change Potentials, among other parameters derived from comprehensive ESMs.

Since its first scientific assessment in 1990, the Intergovernmental Panel on Climate Change (IPCC) has employed the Global Warming Potential (GWP) metric to compare the varying climate impacts arising from emissions of different GHGs [39]. The GWP is the radiative forcing due to a pulse emission of a certain species, integrated over a time horizon,

relative to a pulse emission of carbon dioxide [39], [40]. This metric can serve as a basis to understanding how the AMAP emulator was developed.

In [40] a linearized energy budget is used to define the Absolute Global Temperature Change Potential (AGTP), in units of [K kg^{-1}], as the global average surface temperature change at a time t after a 1 kg pulse emission at time $t = 0$. This study, in addition to [41] and [42], employed this metric to compare the impacts of different pollutants on Earth's mean surface temperature.

The Absolute Regional Temperature-Change Potential (ARTP) is an extension of the AGTP concept, and is employed in the AMAP emulator for simulating regional temperature changes [11], [43], [44]. Additionally, the emulator simulates the heat transport between the 4 geographical regions. As the emulator runs, it generates a temperature response in region m, to a radiative forcing in region l, where $l, m = 1, ..., M$, for the $M = 4$ separate regions, and adds the contributions for a net effect [1].

The ARTP for a region m is defined as follows, in [K kg^{-1}]:

$$ARTP_m(H) = AGTP(H)g\left(\frac{1}{\lambda\delta F_0}\right)RTP_m, \tag{1}$$

where H is the annual time horizon: the elapsed time between the time of the pulse emission and temperature response. g is a dimensionless scaling parameter. δF_0 represents the global radiative forcing perturbation due to all of the pulse emissions, and λ represents the ECS parameter, in [K/W$\cdot m^2$].

The Regional Temperature-Change Potential (RTP) in region m, in [K], is defined as:

$$RTP_m = \sum_{l=1}^{M} k_{lm}\delta F_{0l} \tag{2}$$

where k_{lm} is a matrix of regional temperature response coefficients [K/W$\cdot m^2$]. The values in this matrix were used from simulations with GISS-ER, a coupled atmosphere–ocean climate model [43]. The matrix exists for each of the simulated climate forcers, and are used for different forcing processes, based on the approach used in a previous AMAP BC and O_3 assessment [45]. The λ and δF_0 terms in equation 1 ensure that the ECS value as shown in equation 4 matches the global climate sensitivity calculated from integrating the RTPS:

$$ECS_{RTP} = \frac{F_{2x}}{\delta F_0} \sum_m \sum_l k_{lm} \delta F_{0l} z_m \tag{3}$$

$$ECS = \lambda F_{2x} \tag{4}$$

where F_{2x} is the global radiative forcing from doubling of CO2 and z_m is the global area fraction of region m [$m^2 m^{-2}$].

Currently, the ECS parameter λ in the AMAP emulator is scaled by a coefficient g that brings the ECS from 2.7 K to the derived value of 3.7 K from CMIP6, which also matches recent literature [1], [14], [46], [47], [23]. The ECS would be underestimated without this scaling because the coefficient matrix used to define the RTPs, using values from GISS-ER, were found to produce a lower ECS of 2.7 K. The scaling done in the AMAP emulator is shown in the equation below:

$$g = \frac{\lambda F_{2x}}{ECS_{RTP}} \tag{5}$$

In the AMAP emulator, the ARTP is used to compute and combine regional temperature responses to series of time-varying pulse emissions, resulting in a series of ARTPs with various time horizons as the number of simulated years increases. These ARTPs are summed to estimate the net regional temperature response in region m to annual mean emissions over N, beginning with year t_0 [1]. The total temperature response to emissions of multiple species from the 4 regions are calculated by summing forced temperature changes.

CH_4 is treated by the emulator as a well-mixed GHG without any spatial structure in radiative forcings or dependence on regional emission sources [1]. Its atmospheric lifetime, τ_{CH_4} is modeled as a function of the time scales of other processes:

$$\frac{1}{\tau_{CH_4}} = \frac{1}{\tau_{OH}} + \frac{1}{\tau_{strat}} + \frac{1}{\tau_{soil}} + \frac{1}{\tau_{trop-Cl}} \tag{6}$$

where τ_{OH} is the timescale for CH_4 being destroyed by hydroxyl (OH) radicals, τ_{strat} is the timescale for CH_4 destruction in the stratosphere, τ_{soil} is the time scale for CH_4 uptake by soil, and $\tau_{trop-Cl}$ is the timescale for its reaction with tropospheric chlorine. Each of the contributions are shown in Table 2, resulting in a lifetime of CH_4 of 9.13 years. While natural

Time scale	AMAP Emulator value [yr]
τ_{OH}	11.17
τ_{strat}	120
τ_{soil}	150
$\tau_{trop-Cl}$	200
τ_{CH4}	9.13

Table 2: Time scales of CH_4 loss processes accounted for in its atmospheric lifetime in the AMAP emulator, following [48], [49], [50], and [51].

emissions of CH_4 are included in the emulator, using results from [48], the feedback loop of increased methane concentrations, permafrost thaw, and increased anaerobic respiration from biogenic CH_4 sources is not presently included in the AMAP emulator [9], [49], [10], [53].

As the simulated temperature response is highly linearized, the results are most accurate close to the baseline year. The default reference year is 2015, and the default time period of interest is 1990-2050. The simulations beginning in 1990 are based on results from a spin-up emulator simulation from 1850-1990 [1].

2.5 Evaluating the AMAP Emulator and other Emulators

A 2022 study of the AMAP emulator compared projections generated by the AMAP emulator to results from CMIP6, focusing on CO_2 and SLCFs [6]. The emulator output for the Arctic region (60°-90°N) corresponding to specified CO_2 emissions from SSPs was compared to results from CMIP6. These results were found to be comparable to the warming unmasking due to sulfate emission reductions projected by the emulator. These reductions are often not available in ESMs. This study suggested that the impact of reducing CO_2 emissions could be greatly offset by the unmasking effect from sulfate emission reductions [6].

The new AMAP emulator and comprehensive emissions scenarios were combined for air pollutants and GHGs to evaluate the effects of emission reductions on climate and human health. It was found that technically feasible emissions reduction scenarios could result in

simultaneous climate and human health benefits [6].

In 2022, [7] performed an evaluation of 18 state-of-the-art models and their performance for simulating SLCFs. These models included ESMs, RCMs, CTMs (Chemical Transport Models), Chemistry-Climate Models (CCMs), and GCMs (General Circulation Models). The ways these models represent SLCFs in the Arctic and Northern Hemisphere were evaluated by comparing the results of simulations over 4-year periods (2008–2009 and 2014–2015) from these models to observational data. Though not each model included the same set of species, BC, CH_4, sulfate, tropospheric O_3 and its precursors, organic aerosols, and particulate matter were included when possible for each model.

Absolute and relative model biases were used as the primary metric for evaluating the model output, including annual means, seasonal cycles, and 3-D distributions. The multi-model mean was able to represent the general features of SLCFs in the Arctic and had the best overall performance. For CH_4, O_3, BC, and sulfate, which have great radiative impacts, the multi-model mean was within $\pm 25\%$ of the measurements across the Northern Hemisphere. This demonstrated that using a multi-model ensemble to simulate the climate and health impacts of SLCFs would be optimal.

2.6 Synthesis

SLCFs can have a great impact on human health and climate change, particularly in the Arctic [3], [4]. Comprehensive ESMs are used to simulate projected warming and air quality, but are computationally expensive, so less resource-intensive alternatives for climate and air quality are highly useful, especially for policy-making settings [2], [3], [1]. Effects of SLCFs on climate and their associated feedbacks (ie, cloud-related feedbacks) require a more focused study, as some of these radiative impacts and feedbacks are a high source of uncertainty in climate modelling [14], [52]. The AMAP emulator is a new tool that can be used to simulate projected air quality and climate for various emissions scenarios, but it has limitations, such as its underestimation of Arctic amplification, and very simple model of atmospheric CH_4 [1], [6]. Improvements to the emulator on these aspects are the focus of this study.

3 Progress To Date

3.1 AMAP Emulator vs. CMIP6 Projections

A comparison of Arctic and global AMAP emulator projections to CMIP6 results for various emissions scenarios was conducted to verify and diagnose inconsistencies between the AMAP emulator and the most recent, cutting-edge comprehensive ESMs. This comparison approach is identical to the approach taken for the comparison between AMAP emulator and CMIP6 results conducted in [6], but the points of comparison are different, and an extra scenario (SSP1-1.9) was added. This comparison included nine scenarios, including SSP1-1.9, SSP1-2.6, SSP2-4.5, SSP3-7.0, SSP5-8.5, and four "AMAP" scenarios that focus on mitigating tropospheric O_3 precursors, CH_4, and particulate matter. The SSP nomenclature begins with the umbrella scenario followed by the expected radiative forcing in 2100, in [W m^{-2}], so SSP5-8.5, a fossil-fuel development scenario, is the scenario most impacted by global warming, with an expected radiative forcing of 8.5 W m^{-2} in 2100 [25]. The four AMAP scenarios are described below. For each of these scenarios, the CO_2 emissions follow SSP2-4.5, except for the MFR scenario, which follows SSP1-2.6 for CO_2 emissions [6].

The Current LEgislation (CLE) Scenario includes a complete implementation of national and regional air pollution legislation in addition to existing Nationally Determined Contributions (NDC, as of 2018). This scenario is similar to the SSP2-4.5 scenario, with close reductions in global particulate matter [6].

The Maximum technically Feasible Reduction (MFR) involves global use of the lowest possible air pollutant emissions with no constraints to the associated investment costs but accounting for the lifetime of existing, currently installed equipment and the feasibility of new installations. This idealized scenario involves quicker, steeper reduction of particulate matter species than any of the SSP scenarios [6].

The MFR Sustainable Development (MFR_SDS) scenario includes MFR policies and the Sustainable Development Scenario if the International Energy Agency [6].

The Climate Forcing Mitigation (CFM) scenario includes new policies that focus on CH_4 and warming SLCFs, and assumes CLE policies for the remaining species [6].

The "AMAP" scenarios were not simulated for the sake of comparison with CMIP6

results, as these scenarios are not included in CMIP6. These scenarios were run and plotted for comparison with the results from [6], to check for consistency, which was verified.

The resulting mean surface air temperature difference from each of the nine scenarios were normalized to be relative to 1995-2014 from their original reference to the year 1750. This is the reference time period of the ESM simulations in CMIP6, which allows for direct comparisons between the CMIP6 results and AMAP emulator output for the SSPs. This was completed for the aerosols, CO_2, and CH_4 components of the emulator. For each of these scenarios, an ensemble for each of the forcing agents was created to estimate the uncertainties of the projections. The ensemble for the gas species projections included a range of ECS values, including $ECS = \{2.59, 3.70, 5.00\}$. Ensembles for the aerosols included these three ECS values as well as two perturbation values (a high and a low value) for aerosol/cloud interactions, aerosol/radiation interactions, and aerosol/snow interactions. These values were the same as used in [6].

The normalized AMAP emulator projections until 2030 and 2050 were compared to results from CMIP6, specifically the subset of ESMs from CMIP6 that had ECS values of $2.5 < ECS < 4.0$ K, based on the results from the IPCC Sixth Assessment Report and other recent studies [6], [13], [52].

The results for the comparison until 2050 are shown in Figure 1, and the comparison for 2030 is shown in Figure 2. Table 3 shows corresponding numerical the mean relative difference of the results across the SSPs for each region/year combination. The mean relative difference Δ_{rel} is defined in equation 7, where there are $N = 5$ SSP scenarios, and x_i and y_i represent the estimated temperature difference from the AMAP emulator and CMIP6 results, respectively.

$$\Delta_{rel} = \frac{1}{N} \sum_{i=1}^{N} \frac{x_i - y_i}{(x_i + y_i)/2} \cdot 100\% \tag{7}$$

In 2050, the Global SSP results are in worse agreement than the results from the Arctic latitude band of 60°N - 90°N. For 2050, there is an overall trend of Arctic warming being underestimated by the AMAP emulator, as the mean relative difference was found to be $-22.4 \pm 27.0\%$. This is in accordance with the findings from [6], which included a highly similar comparison between AMAP emulator and CMIP6 results, but with a larger set of

Year	Region	Δ_{rel}
2030	Arctic	-5.0 ±31.5%
2030	Global	20.5 ±15.7%
2050	Arctic	-22.4 ±27.0%
2050	Global	19.3 ±16.0%

Table 3: Coefficients of variance corresponding to Figures 2 and 1.

ESMs from CMIP6 included. This underestimation of Arctic warming is less evident in Figure 2, which shows projection results until 2030, which shows a much smaller but still negative mean relative difference of $-5.0 \pm 31.5\%$. The uncertainties of these comparisons are extremely high to to the propagated uncertainties from the CMIP6 and AMAP results.

A notable outlier from the 2030 comparison, in Figure 2(d) is that the projected warming is underestimated by AMAP compared to CMIP6 much more for SSP1-1.9 than for the other scenarios, which include relative differences that are both positive and negative. This may be due to a bias from a particular species in the SSP1-1.9, but this has not yet been investigated. A breakdown of CMIP6 results by molecule would assist in understanding the possible biases in the projections for each species from the AMAP emulator.This could also help to inform modifications to the Arctic RTP for each species.

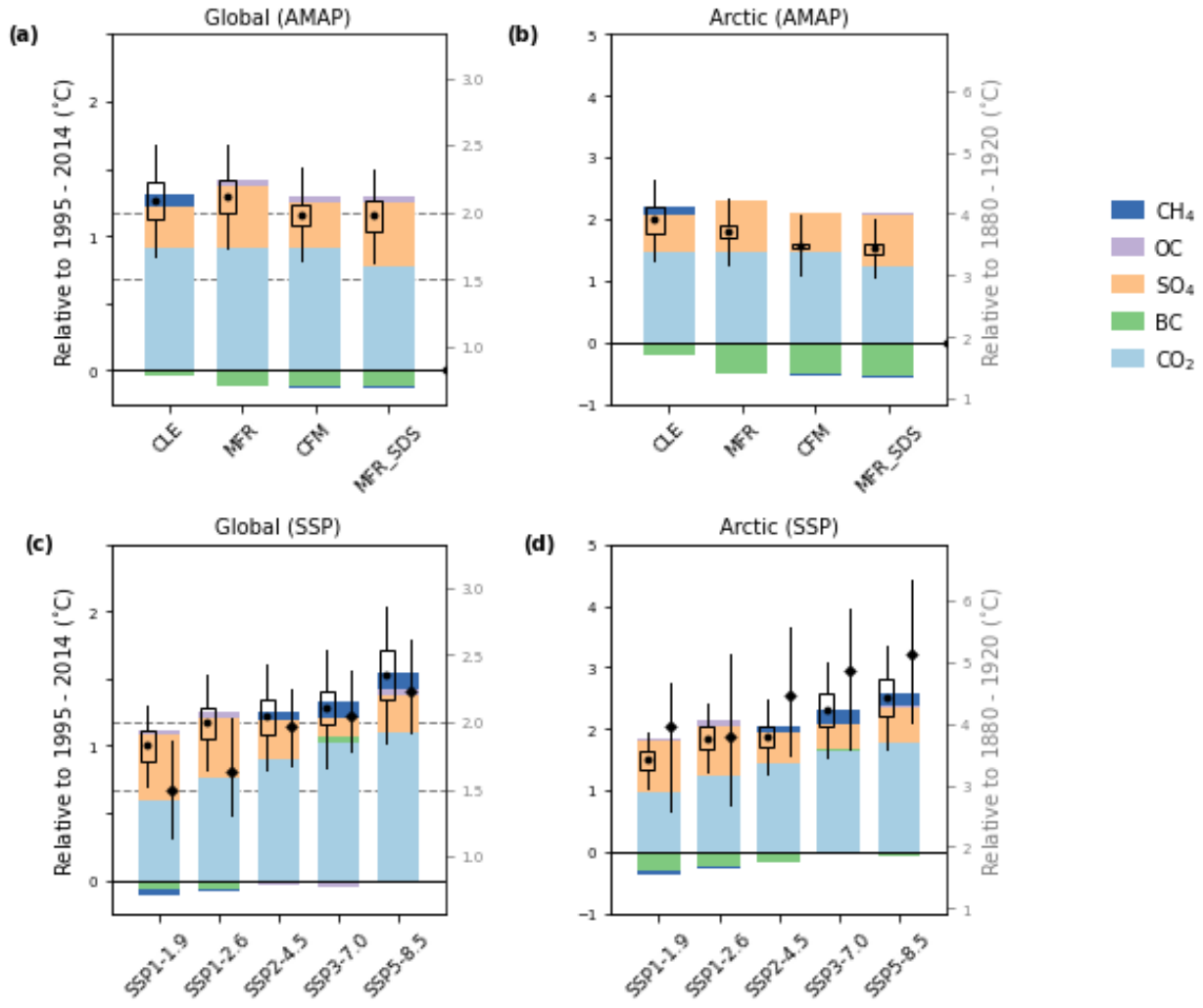

Figure 1: Projected global and Arctic mean surface temperature changes in 2050. The net temperature changes projected by the AMAP emulator are plotted as circles, the CMIP6 multi-model median values as diamonds. The 5–95% confidence intervals ($\pm 1.64\sigma$), resulting from uncertainties in all simulated processes, are shown as black error bars. Confidence ranges from to radiative forcing uncertainty in the AMAP emulator are shown as transparent rectangles. Color bars refer to the forced temperature change from the individual air pollutant and greenhouse gas species, based on AMAP emulator simulations (see legend). (a) and (b) only show results from the AMAP emulator, as the AMAP scenarios are plotted. Confidence ranges due to radiative forcing uncertainty in the emulator are indicated by transparent rectangles. Warming relative to preindustrial conditions is also indicated (grey font, with 1.5 and 2 °C thresholds indicated by dashed lines in (a), (c)).

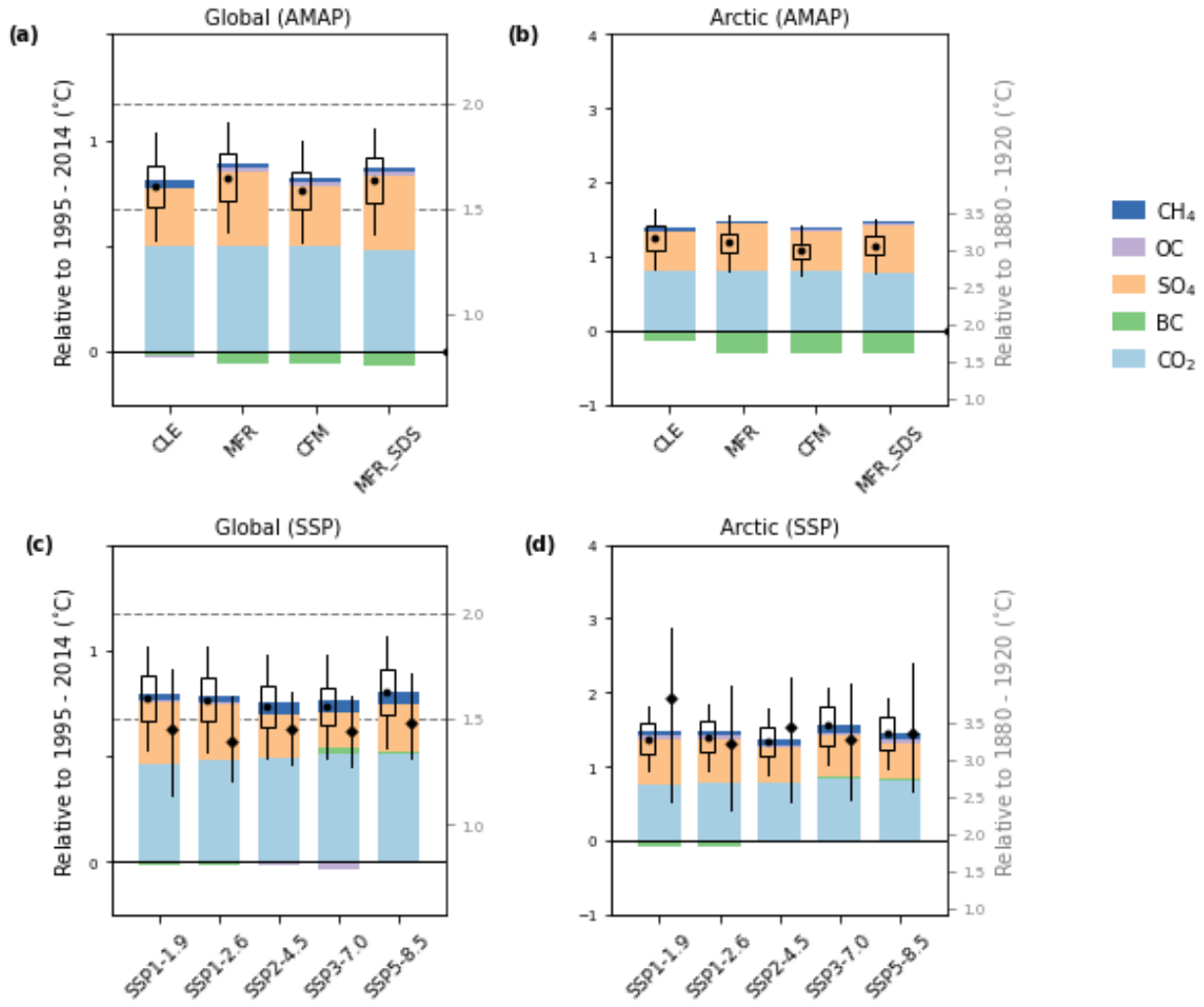

Figure 2: Same as Figure 1, but for the year 2030.

4 Future Work

4.1 Work Plan

An outline of the weekly progress scheduled for the remainder of the term is is shown in Table 4.

The three main objectives of the study are partitioned according to each week. These include the modification of the AMAP emulator's RTP coefficients to better emulate Arctic temperatures, adapting CH_4's representation in the emulator (adapting its atmospheric lifetime to better match CMIP6 result and adding a temperature feedback loop), and using the AMAP emulator output to study the effects of BC on climate indicators such as Arctic sea ice.

The first goal is to modify the existing RTP coefficients to better match the CMIP6 results. As discussed, the coefficients from GISS-ER that were used to generate the RTPs result in an ECS of 2.7°C that is scaled up to 3.7°C to match recent studies [1], [14][46], [47], [23]. The coefficients for the Arctic RTP require modification. Specifically, to improve the emulator to better match more recent comprehensive models, the emulator output will be compared against the CMIP6 results shown in Figures 1 and 2. The comparisons performed thus far have not included O_3, but the AMAP emulator has O_3 projecting capabilities, so future comparisons could include this species to better match CMIP6 results and to better emulate Earth's atmosphere. The causes of outliers in the comparisons performed so far will be investigated, specifically which species could have caused SSP-specific biases in the AMAP/CMIP6 prediction differences.

The coefficients will be scaled up by a coefficient Δ with an area-weighted decrease in the coefficients for the other regions. The resulting ECS value from the RTPs will thus be increased to a value closer to the value of 3.7°C that it is manually adjusted to by the coefficient g in equation 5. The mean relative difference in projected mean surface air temperature change, Δ_{rel}, and the coefficient of variation will be used as metrics for quantifying how well the AMAP emulator output captures the CMIP6 results for both 2030 and 2050 results, for each latitude band of the emulator.

After the modified RTPs have been finalized, the CH_4 atmospheric lifetime will be updated. This may include modifying certain components or adding new factors to its atmospheric lifetime, as shown in equation 6. Additionally, a simple feedback loop linking CH_4 emissions and Arctic temperature (ie, due to permafrost thaw) will be added. The feedback loop of increased CH_4 concentrations, permafrost thaw, and increased anaerobic respiration from biogenic CH_4 sources is not presently included in the AMAP emulator [9], [10], [49],

Date	Project Tasks
Jan 30 – Feb 5	- Preliminary testing of RTP coefficients for the Arctic.
Feb 6 – 12	- Test for the 5 provided SSPs and draw comparison with CMIP6 results. - Do comparisons on a regional scale when the data becomes available. - Approach tuning other RTPs (NH, SH, Antarctica).
Feb 13 – 19	- Finalizing new RTP coefficients. - Reading on CH_4 feedback loops and natural emissions, specifically how they are modelled in emulators where applicable.
Feb 20 – 26	- Tweaking atmospheric lifetime of CH_4.
Feb 27 – Mar 5	- Incorporating natural emissions of CH_4 to account for the potential increase in anaerobic respiration as a natural methane source.
Mar 6 – 12	- Run emulator with different CH_4 emissions, ie. 5 SSPs.
Mar 13 – 19	- Studying the effects of BC on Arctic climatology using the emulator.
Mar 20 – 26	- Study particular indicators, ie. how BC affects the sea ice in comparison to other climate forcers (TBD).
Mar 27 – Apr 2	- Editing and reviewing thesis presentation and document.
Apr 3 – Apr 9	- Thesis presentations from Mar. 27 – Apr. 6.
Apr 10 – Apr 14	- Editing and reviewing thesis document. - Submission of final thesis document, due Apr 14.

Table 4: Schedule for future work, until the end of the term, divided by weeks.

[53]. Further research into this mechanism and how it has been represented in recent ESMs and climate emulators will be conducted to inform this addition to the AMAP emulator.

Finally, time-permitting, the emulator will be run for different scenarios to observe and quantify how BC affects the sea ice in comparison to other climate forcers. This aspect of the project will require further research into the effect of BC on Arctic climatology and would require acessing another dataset(s) to draw comparisons and conclusions.

The main deliverables of the project presentation and the final thesis document will be developed throughout the remainder of the term, becoming the primary focus in the final weeks.

References

1. K. von Salzen, "Technical Summary: The AMAP Climate and Air Quality Emulator," 2021.

2. Z. R. J. Nicholls et al., "Reduced Complexity Model Intercomparison Project Phase 1: introduction and evaluation of global-mean temperature response," Geosci. Model Dev., vol. 13, no. 11, pp. 5175–5190, 2020.

3. K. Kupiainen, M. Flanner, and S. Eckhardt, "Climate effects of other pollutants – short-lived climate forcers and the Arctic," Global Arctic, pp. 171–187, 2022.

4. AMAP, Impacts of Short-lived Climate Forcers on Arctic Climate, Air Quality, and Human Health. Summary for Policy-makers. Tromsø, Norway: Arctic Monitoring and Assessment Programme (AMAP).

5. M. Previdi, K. L. Smith, and L. M. Polvani, "Arctic amplification of climate change: A review of underlying mechanisms," Environmental Research Letters, vol. 16, no. 9, p. 093003, 2021.

6. K. von Salzen et al., "Clean air policies are key for successfully mitigating Arctic warming," Earth Environment, 2022.

7. C. H. Whaley, R. Mahmood, K. von Salzen, B. Winter, S. Eckhardt, S. Arnold, S. Beagley, S. Becagli, R.-Y. Chien, J. Christensen, S. M. Damani, K. Eleftheriadis, N. Evangeliou, G. S. Faluvegi, M. Flanner, J. S. Fu, M. Gauss, F. Giardi, W. Gong, J. L. Hjorth, L. Huang, U. Im, Y. Kanaya, S. Krishnan, Z. Klimont, T. Kühn, J. Langner, K. S. Law, L. Marelle, A. Massling, D. Olivié, T. Onishi, N. Oshima, Y. Peng, D. A. Plummer, O. Popovicheva, L. Pozzoli, J.-C. Raut, M. Sand, L. N. Saunders, J. Schmale, S. Sharma, H. Skov, F. Taketani, M. A. Thomas, R. Traversi, K. Tsigaridis, S. Tsyro, S. Turnock, V. Vitale, K. A. Walker, M. Wang, D. Watson-Parris, and T. Weiss-Gibbons, "Model evaluation of short-lived climate forcers for the Arctic Monitoring and Assessment Programme: A multi-species, multi-model study," Preprint. Gases/Atmospheric Modelling/Troposphere/Chemistry (chemical composition and reactions), Nov. 2021.

8. C. H. Whaley, R. Mahmood, K. von Salzen, B. Winter, S. Eckhardt, S. Arnold, S. Beagley, S. Becagli, R.-Y. Chien, J. Christensen, S. M. Damani, X. Dong, K. Eleftheriadis, N. Evangeliou, G. Faluvegi, M. Flanner, J. S. Fu, M. Gauss, F. Giardi, W. Gong, J. L. Hjorth, L. Huang, U. Im, Y. Kanaya, S. Krishnan, Z. Klimont, T. Kühn, J. Langner, K. S. Law, L. Marelle, A. Massling, D. Olivié, T. Onishi, N. Oshima, Y. Peng, D. A. Plummer, O. Popovicheva, L. Pozzoli, J.-C. Raut, M. Sand, L. N. Saunders, J. Schmale, S. Sharma, R. B. Skeie, H. Skov, F. Taketani, M. A. Thomas, R. Traversi, K. Tsigaridis, S. Tsyro, S. Turnock, V. Vitale, K. A. Walker, M. Wang, D. Watson-Parris, and T. Weiss-Gibbons, "Model evaluation of short-lived climate forcers for the Arctic Monitoring and Assessment Programme: A multi-species, multi-model study," Atmospheric Chemistry and Physics, vol. 22, no. 9, pp. 5775–5828, 2022.

9. D. M. Lawrence, C. D. Koven, S. C. Swenson, W. J. Riley, and A. G. Slater, "Permafrost thaw and resulting soil moisture changes regulate projected high-latitude co 2 and CH 4 emissions," Environmental Research Letters, vol. 10, no. 9, p. 094011, 2015.

10. I. S. A. Isaksen, M. Gauss, G. Myhre, K. M. Walter Anthony, and C. Ruppel, "Strong atmospheric chemistry feedback to climate warming from Arctic methane emissions: ARCTIC METHANE FEEDBACK," Global Biogeochem. Cycles, vol. 25, no. 2, 2011.

11. D. Shindell and G. Faluvegi, "The net climate impact of coal-fired power plant emissions," Atmospheric Chemistry and Physics, vol. 10, no. 7, pp. 3247–3260, 2010.

12. A. Stohl et al., "Evaluating the climate and air quality impacts of short-lived pollutants," Atmos. Chem. Phys., vol. 15, no. 18, pp. 10529–10566, 2015.

13. https://www.ipcc.ch/report/ar6/wg1/chapter/chapter-6/.

14. G. A. Meehl et al., "Context for interpreting equilibrium climate sensitivity and transient climate response from the CMIP6 Earth system models," Sci. Adv., vol. 6, no. 26, p. eaba1981, 2020.

15. J. Alcamo, M. Krol, and M. Posch, "An integrated analysis of sulfur emissions, acid deposition and climate change," Water Air Soil Pollut., vol. 85, no. 3, pp. 1539–1550, 1995.

16. G. A. Ban-Weiss, L. Cao, G. Bala, and K. Caldeira, "Dependence of climate forcing and response on the altitude of Black Carbon Aerosols," Climate Dynamics, vol. 38, no. 5-6, pp. 897–911, 2011.

17. World Health Organization, "Ambient air pollution: a global assessment of exposure and burden of disease," Clean Air J., vol. 26, no. 2, p. 6, 2016.

18. M. Brauer et al., "Exposure assessment for estimation of the global burden of disease attributable to outdoor air pollution," Environ. Sci. Technol., vol. 46, no. 2, pp. 652–660, 2012.

19. J. Lelieveld, J. S. Evans, M. Fnais, D. Giannadaki, and A. Pozzer, "The contribution of outdoor air pollution sources to premature mortality on a global scale," Nature, vol. 525, no. 7569, pp. 367–371, 2015.

20. R. J. Allen et al., "Significant climate benefits from near-term climate forcer mitigation in spite of aerosol reductions," Environ. Res. Lett., 2021.

21. J. Lelieveld, K. Klingmüller, A. Pozzer, R. T. Burnett, A. Haines, and V. Ramanathan, "Effects of fossil fuel and total anthropogenic emission removal on public health and climate," Proc. Natl. Acad. Sci. U. S. A., vol. 116, no. 15, pp. 7192–7197, 2019.

22. D. Shindell et al., "Simultaneously mitigating near-term climate change and improving human health and food security," Science, vol. 335, no. 6065, pp. 183–189, 2012.

23. M. D. Zelinka et al., "Causes of higher climate sensitivity in CMIP6 models," Geophys. Res. Lett., vol. 47, no. 1, 2020.

24. Z. Nicholls et al., "Reduced Complexity Model Intercomparison Project Phase 2: Synthesizing earth system knowledge for probabilistic climate projections," Earths Future, vol. 9, no. 6, p. e2020EF001900, 2021.

25. K. Riahi et al., "The Shared Socioeconomic Pathways and their energy, land use, and greenhouse gas emissions implications: An overview," Glob. Environ. Change, vol. 42, pp. 153–168, 2017.

26. M. Meinshausen, S. C. B. Raper, and T. M. L. Wigley, "Emulating coupled atmosphere-ocean and carbon cycle models with a simpler model, MAGICC6 – Part 1: Model description and calibration," Atmos. Chem. Phys., vol. 11, no. 4, pp. 1417–1456, 2011.

27. P. Good, J. M. Gregory, and J. A. Lowe, "A step-response simple climate model to reconstruct and interpret AOGCM projections: A STEP-RESPONSE SIMPLE CLIMATE MODEL," Geophys. Res. Lett., vol. 38, no. 1, 2011.

28. O. Geoffroy, D. Saint-Martin, D. J. L. Olivié, A. Voldoire, G. Bellon, and S. Tytéca, "Transient climate response in a two-layer energy-balance model. Part I: Analytical solution and parameter calibration using CMIP5 AOGCM experiments," J. Clim., vol. 26, no. 6, pp. 1841–1857, 2013.

29. P. M. Forster, A. C. Maycock, C. M. McKenna, and C. J. Smith, "Latest climate models confirm need for urgent mitigation," Nat. Clim. Chang., vol. 10, no. 1, pp. 7–10, 2020.

30. C. J. Smith et al., "FAIR v1.1: A simple emissions-based impulse response and carbon cycle model," 2017.

31. T. Gasser et al., "The compact Earth system model OSCAR v2.2: description and first results," Geosci. Model Dev., vol. 10, no. 1, pp. 271–319, 2017.

32. K. M. Foley, S. L. Napelenok, C. Jang, S. Phillips, B. J. Hubbell, and C. M. Fulcher, "Two reduced form air quality modeling techniques for rapidly calculating pollutant mitigation potential across many sources, locations and precursor emission types," Atmos. Environ. (1994), vol. 98, pp. 283–289, 2014.

33. J. Li et al., "A modeling study of source–receptor relationships in atmospheric particulate matter over Northeast Asia," Atmos. Environ. (1994), vol. 91, pp. 40–51, 2014.

34. Y. Liu et al., "Source-receptor relationships for PM2.5 during typical pollution episodes in the Pearl River Delta city cluster, China," Sci. Total Environ., vol. 596–597, pp. 194–206, 2017.

35. P. S. Porter, S. T. Rao, C. Hogrefe, and R. Mathur, "A reduced form model for ozone based on two decades of CMAQ simulations for the continental United States," Atmos. Pollut. Res., vol. 8, no. 2, pp. 275–284, 2017.

36. R. Van Dingenen et al., "TM5-FASST: a global atmospheric source-receptor model for rapid impact analysis of emission changes on air quality and short-lived climate pollutants," Atmos. Chem. Phys. Discuss., pp. 1–55, 2018.

37. J. Tsutsui, "Quantification of temperature response to CO2 forcing in atmosphere–ocean general circulation models," Clim. Change, vol. 140, no. 2, pp. 287–305, 2017.

38. "About," Amap.no. [Online]. Available: https://www.amap.no/about.

39. The Intergovernmental Panel on Climate Change (IPCC): 1990, Climate Change: The Intergovernmental Panel on Climate Change Scientific Assessment. Cambridge, UK: Cambridge University Press.

40. K. P. Shine, J. S. Fuglestvedt, K. Hailemariam, and N. Stuber, "Alternatives to the global warming potential for comparing climate impacts of emissions of greenhouse gases," Clim. Change, vol. 68, no. 3, pp. 281–302, 2005.

41. O. Boucher and M. S. Reddy, "Climate trade-off between black carbon and carbon dioxide emissions," Energy Policy, vol. 36, no. 1, pp. 193–200, 2008.

42. J. S. Fuglestvedt et al., "Transport impacts on atmosphere and climate: Metrics," Atmos. Environ. (1994), vol. 44, no. 37, pp. 4648–4677, 2010.

43. D. Shindell and G. Faluvegi, "Climate response to regional radiative forcing during the twentieth century," Nat. Geosci., vol. 2, no. 4, pp. 294–300, 2009.

44. D. T. Shindell, "Evaluation of the absolute regional temperature potential," Atmos. Chem. Phys., vol. 12, no. 17, pp. 7955–7960, 2012.

45. "Black carbon and ozone as Arctic climate forcers," Arctic Monitoring and Assessment Programme, 2015.

46. G. A. Schmidt et al., "Present-day atmospheric simulations using GISS ModelE: Comparison to in situ, satellite, and reanalysis data," J. Clim., vol. 19, no. 2, pp. 153–192, 2006.

47. F. J. M. M. Nijsse, P. M. Cox, and M. S. Williamson, "Emergent constraints on transient climate response (TCR) and equilibrium climate sensitivity (ECS) from historical warming in CMIP5 and CMIP6 models," Earth Syst. Dyn., vol. 11, no. 3, pp. 737–750, 2020.

48. M. J. Prather, C. D. Holmes, and J. Hsu, "Reactive greenhouse gas scenarios: Systematic exploration of uncertainties and the role of atmospheric chemistry: ATMOSPHERIC CHEMISTRY AND GREENHOUSE GASES," Geophys. Res. Lett., vol. 39, no. 9, 2012.

49. "Atmospheric chemistry and greenhouse gases," in The Scientific Basis. Contribution of Working Group I to the Third Assessment Report of the Intergovernmental Panel on Climate Change, 2001.

50. "Climate change 2013: The physical science basis," in Contribution of Working Group I to the fifth assessment report of the Intergovernmental Panel on Climate Change.

51. A. Voulgarakis et al., "Analysis of present day and future OH and methane lifetime in the ACCMIP simulations," Atmos. Chem. Phys., vol. 13, no. 5, pp. 2563–2587, 2013.

52. Z. Hausfather, K. Marvel, G. A. Schmidt, J. W. Nielsen-Gammon, and M. Zelinka, "Climate simulations: recognize the 'hot model' problem," Nature, vol. 605, no. 7908, pp. 26–29, 2022.

53. S. Kirschke et al., "Three decades of global methane sources and sinks," Nat. Geosci., vol. 6, no. 10, pp. 813–823, 2013.